



**Universiteit  
Leiden**  
The Netherlands

## **Multimodality imaging to guide cardiac interventional procedures**

Tops, L.F.

### **Citation**

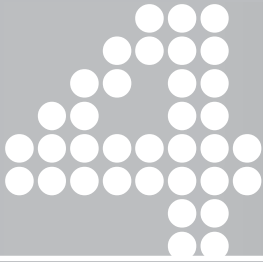
Tops, L. F. (2010, April 15). *Multimodality imaging to guide cardiac interventional procedures*. Retrieved from <https://hdl.handle.net/1887/15228>

Version: Corrected Publisher's Version

License: [Licence agreement concerning inclusion of doctoral thesis in the Institutional Repository of the University of Leiden](#)

Downloaded from: <https://hdl.handle.net/1887/15228>

**Note:** To cite this publication please use the final published version (if applicable).



# **Fusion of multi-slice computed tomography imaging with three-dimensional electroanatomical mapping to guide radiofrequency catheter ablation procedures**

Laurens F. Tops<sup>1</sup>

Jeroen J. Bax<sup>1</sup>

Katja Zeppenfeld<sup>1</sup>

Monique R.M. Jongbloed<sup>1</sup>

Hildo J. Lamb<sup>2</sup>

Ernst E. van der Wall<sup>1</sup>

Martin J. Schalij<sup>1</sup>

<sup>1</sup>*Department of Cardiology, Leiden University Medical Center, Leiden, the Netherlands*

<sup>2</sup>*Department of Radiology, Leiden University Medical Center, Leiden, the Netherlands*

*Heart Rhythm 2005;2:1076-81*

## ABSTRACT

**Background:** The outcome of catheter ablation procedures of cardiac arrhythmias depends on the ability to evaluate the underlying mechanism and to depict target sites for ablation. Fusion of different imaging modalities within one system may improve electroanatomic modeling and facilitate ablation procedures.

**Objectives:** To study the feasibility of fusion of multi-slice computed tomography (MSCT) with electroanatomic mapping to guide radiofrequency catheter ablation of atrial arrhythmias.

**Methods:** Sixteen patients (15 men, age  $54 \pm 7$  years) with drug-refractory atrial fibrillation (AF) underwent 64-slice MSCT within 2 days before radiofrequency catheter ablation. MSCT data were imported in the Carto™ electroanatomic mapping system. Using the new CartoMerge™ Image Integration Module, the MSCT images and the electroanatomical map were aligned. A statistical algorithm provided information about the accuracy of the fusion process.

**Results:** In all patients MSCT images could be fused with the electroanatomic map. Mean distance between the mapping points and the MSCT surface ranged from  $1.7 \pm 1.2$  mm to  $2.8 \pm 1.8$  mm. This resulted in an average of  $2.1 \pm 0.2$  mm for the patient group as a whole.

**Conclusion:** MSCT images can be fused with the 3D electroanatomic mapping system in an accurate manner. Anatomy-based catheter ablation procedures for atrial arrhythmias may be facilitated by integration of different imaging modalities.

## INTRODUCTION

Ectopic beats originating from the pulmonary veins have been identified as a potential cause of atrial fibrillation (AF) (1). Catheter ablation focused on isolation of the pulmonary veins is a curative treatment modality of AF. Different strategies for pulmonary vein isolation have been proposed, including segmental (2) and circumferential (3) ablation. Electrical isolation of the pulmonary veins has proved to be a safe technique with a reasonable long-term success rate (4,5). To plan and guide these ablation procedures, detailed anatomic information is needed. Several imaging modalities are available to visualize the anatomy of the left atrium and the pulmonary veins.

Both magnetic resonance imaging and multi-slice computed tomography (MSCT) are non-invasive imaging modalities that can provide the requested information and both imaging modalities have been used to provide road maps prior to ablation (6,7). These techniques provide detailed information on the precise number, location and anatomy of the pulmonary veins and have been demonstrated useful in the planning of ablation procedures (8,9). In addition, detailed information is also needed during the ablation procedure; fluoroscopy alone is not accurate enough and may result in a prolonged radiation exposure. For this purpose, 3D electroanatomic mapping systems that facilitate ablation procedures have been introduced (10). However, a realistic anatomical representation of the left atrium and pulmonary veins is still difficult to obtain. Therefore, fusion of an anatomical imaging technique (e.g. MSCT) with 3D electroanatomic mapping may further facilitate ablation procedures. In the current study, the feasibility of fusion of MSCT with electroanatomic mapping is demonstrated in patients undergoing radiofrequency ablation for AF.

## METHODS

### Study population

The study population consisted of 16 consecutive patients (15 men, mean age  $54 \pm 7$  years) with symptomatic drug-refractory AF who were admitted for radiofrequency catheter ablation. AF was present for  $54 \pm 12$  months, and was paroxysmal in 5 patients, persistent in 9 and permanent in 2 patients. Mean number of anti-arrhythmic drugs used was  $3.7 \pm 1.6$  per patient. Mean left atrial size was  $4.4 \pm 0.3$  cm; mean left ventricular ejection fraction was  $57 \pm 10\%$ . Seven patients were treated for hypertension; none of the patients had clinically relevant valvular disease. Six patients underwent coronary angiography for suspected coronary artery disease; in none of the patients significant coronary artery stenoses were detected. One patient had a pacemaker. In two patients a catheter ablation procedure for atrial flutter was performed previously.

### **Multi-slice computed tomography**

All patients underwent MSCT using a 64-detector row system (Toshiba Medical Systems, Otawara, Japan) 2 days prior to the ablation procedure, as previously reported (8). Collimation was 64 x 0.5 mm, rotation time 400 ms, and tube voltage 100 kV at 250 mA. Cranio-caudal scanning was performed during an inspiratory breathhold, without electrocardiographic gating. Non-ionic contrast material (Iomeron 400, Bracco Altana Pharma, Konstanz, Germany) was infused through the antecubital vein with an infusion rate of 5 ml/s. A total amount of 70 ml contrast was given. Automatic detection of the contrast bolus in the ascending aorta was used to time the scan. All MSCT images were evaluated by two experienced observers in consensus. To assess the number of pulmonary veins, the number of ostia (common or separate ostia), and the branching pattern of the pulmonary veins, 2D viewing modes and 3D reconstructions were used. Diameters of the pulmonary vein ostia were measured in the anterior-posterior and superior-inferior direction, as previously described (8). Furthermore, thrombi in the left atrial appendage and extra-cardiac anomalies were excluded.

### **Image processing**

Before the ablation procedure, raw MSCT data were loaded into the 3D electroanatomic mapping system (Carto XP™, Biosense Webster, California, USA) equipped with the newly developed CartoMerge™ Image Integration Module. The accuracy of this new technique has been validated in animal studies previously (11). To depict the structures of interest (left atrium and pulmonary veins) out of the raw data set, a segmentation process was performed manually.

This process consisted of several phases. First, the borders of the structures of interest were delineated by setting the threshold intensity range. The presence of contrast in the left atrium allowed differentiation between endocardium (low intensity level) and blood pool (high intensity level). Subsequently, a 3D volume was created by labeling all volume units of the raw MSCT data within the set threshold intensity range. To segment this volume into different structures, anatomical markers were placed in the middle of the different areas of the volume. An algorithm was then implemented to automatically depict the different structures of interest based on the placement of the anatomical markers and the borders (Figure 1). Finally, the result of the segmentation process was verified on axial slices. When an adequate segmentation of the MSCT images was achieved, the surface images were stored in the Carto™ system.

### **Mapping and radiofrequency ablation**

The aim of the radiofrequency catheter ablation procedure for AF was to obtain an electrical disconnection of all pulmonary veins. With the use of intracardiac echocardiography an intracardiac thrombus was excluded and a transseptal puncture was guided (12). Mapping and ablation was performed with a 4 mm quadripolar mapping/ablation catheter (7F Thermocool, Biosense Webster, California, USA). A 6F reference catheter was placed in the right atrium.

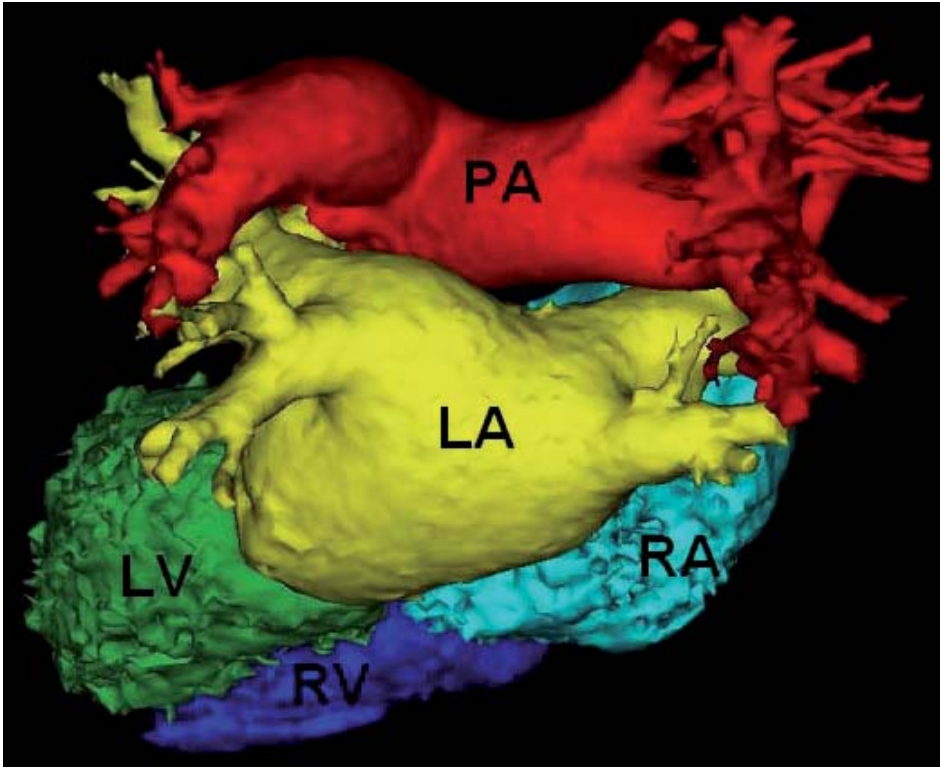


**Figure 1.** Multislice computed tomography image after segmentation using the CartoMerge™ Image Integration Module. Segmentation included: creation of a 3D volume, placement of anatomical markers on different structures and implementation of an algorithm that creates the different structures of interest (see text). LA = left atrium; LV = left ventricle; PA = pulmonary arteries; RA = right atrium; RV = right ventricle.

After completion of the electroanatomic map, a registration process was performed manually to fuse the MSCT images and the electroanatomic map. First, the 3D surface image of the MSCT was displayed on the Carto™ system next to the electroanatomic map. A landmark was then placed on the electroanatomic map on a certain point (e.g. left atrial appendage), confirmed with intracardiac echocardiography and fluoroscopy. A second landmark was placed on the MSCT image at the same location (Figure 2). Next, the surface registration algorithm was performed to align the MSCT surface image and the electroanatomic map. This algorithm composed the best fit of the two structures based on minimizing distance between the two landmarks and the distance between all mapping points and the MSCT surface image.

The accuracy of the registration process was then reviewed. The algorithm used for fusion provided information about the accuracy of the registration: mean distance, standard deviation and range between all mapping points and the MSCT surface image were reviewed. Furthermore, the catheter position in the fused electroanatomic map and MSCT was reviewed using intracardiac echocardiography and fluoroscopy.

After registration of the MSCT surface image radiofrequency current was applied outside the ostia of the pulmonary veins, using the ablation catheter with a 4 mm open loop irrigated

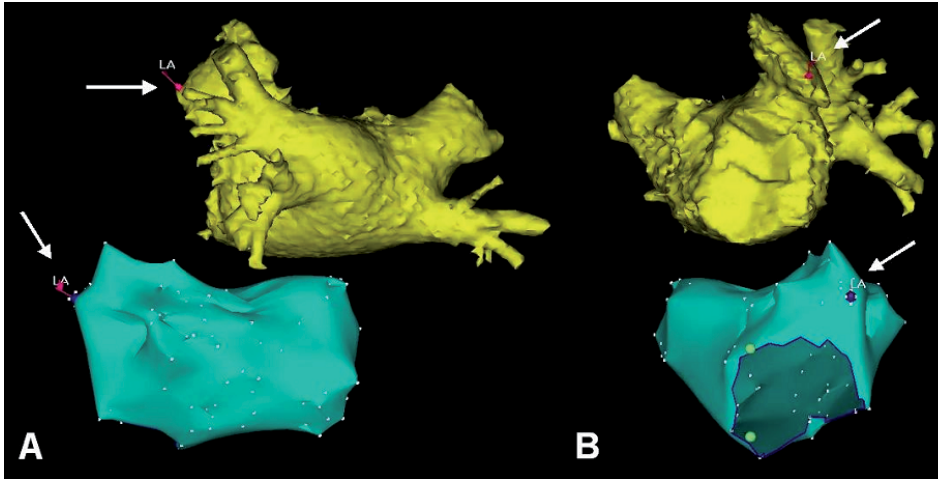


**Figure 2.** During the ablation procedure, a registration process was performed to fuse the electroanatomic map and the MSCT image. After completion of the electroanatomic map of the left atrium, landmarks were placed on the electroanatomic map and the MSCT surface image. In this case, a landmark (LA) was placed on the left atrial appendage, based on fluoroscopy and intracardiac echocardiography. Panel A: posterior view, Panel B: lateral view.

tip. The following power and temperature settings were used: irrigation rate 20 mL/min, maximum temperature 50°C, maximum radiofrequency energy 30 W. At each point, radiofrequency current was applied until a voltage <0.1 mV was achieved, with a maximum of 60 seconds per point. If a separate pulmonary venous insertion was noted on the MSCT image, radiofrequency current was targeted to form separate circles surrounding the pulmonary venous ostia. If a common ostium was observed, ablation points were targeted in a large circle surrounding the common ostium. The procedure was considered successful when pulmonary vein isolation was confirmed by recording entrance block during sinus rhythm or pacing in the coronary sinus. All patients received heparin intravenously (activated clotting time > 300 sec) to avoid thromboembolic complications.

After the ablation procedure, patients received heparin intravenously until INR was adequate with oral anticoagulants. Transthoracic 2D echocardiography was performed within 24 hours to detect pericardial effusion. Electrocardiographic monitoring (including 12-lead surface and 24-hour Holter monitoring) was obtained to assess the maintenance of sinus rhythm after the ablation procedure.

### Statistical analysis

The statistical algorithm of the new CartoMerge™ Image Integration Module provides statistical information (mean, standard deviation and range) about the distances between all mapping points and the MSCT surface image. All data are presented as mean ± standard deviation or number (%).

## RESULTS

### MSCT and image processing

In the 16 patients, a total number of 67 pulmonary veins were identified by MSCT ( $4.2 \pm 0.4$  per patient). In 3 patients (19%), an additional pulmonary vein on the right side was observed. A common ostium of the left-sided pulmonary veins was noted in 6 patients (38%), and a common ostium of the right-sided pulmonary veins in 1 patient (6%). In 9 patients (63%), early branching pattern of a pulmonary vein was observed, all in the right inferior pulmonary vein.

The anterior-posterior and superior-inferior diameters were as follows: left superior pulmonary vein  $15.8 \pm 2.3$  mm and  $19.0 \pm 2.1$  mm respectively, left inferior pulmonary vein  $13.2 \pm 2.0$  mm and  $18.4 \pm 1.9$  mm, right superior pulmonary vein  $17.7 \pm 2.7$  mm and  $20.1 \pm 3.3$  mm, right inferior pulmonary vein  $17.3 \pm 2.7$  mm and  $17.6 \pm 2.4$  mm, respectively.

Image processing of the raw MSCT data could be performed within 10 minutes in all patients. Good contrast timing during the CT scan favored the segmentation process: the presence of contrast allowed excellent differentiation between the endocardium (low intensity level) and the blood pool (high intensity level). In all patients, an adequate segmentation of the MSCT was achieved.

### Mapping and radiofrequency ablation

Eventually, all patients were treated with radiofrequency catheter ablation for AF. In all patients a transseptal puncture could be performed guided by intracardiac echocardiography. Mean mapping time was  $43 \pm 15$  minutes, and a mean of  $224 \pm 59$  mapping points was used to create an electroanatomic map of the left atrium and pulmonary veins. There was no difference in heart rhythm during MSCT scanning and the mapping / ablation procedure.

After placement of the landmarks, the MSCT image and the electroanatomic map were fused. This registration process could be performed within 5 - 7 minutes in all patients. After the registration, the distances between all mapping points and the MSCT surface image were reviewed. Results of the registration processes are listed in Table 1. Mean distance between the mapping points and the MSCT surface ranged from  $1.7 \pm 1.2$  mm to  $2.8 \pm 1.8$  mm. This resulted in an average of  $2.1 \pm 0.2$  mm for the patient group as a whole.

The fused electroanatomic map and MSCT surface image were used to guide the catheter during the actual ablation. Exact catheter position and relation to the pulmonary veins and the endocardium could be adequately visualized (Figure 3). Radiofrequency current was applied outside the ostia of all the pulmonary veins. Mean ablation time was  $89 \pm 20$  minutes, and mean fluoroscopy time was  $48 \pm 7$  minutes. Procedural success was achieved in all patients. No complications occurred during the ablation procedures, in 2 patients mild pericardial effusion was observed after the procedure, without hemodynamic consequences. After the ablation procedure all patients were in sinus rhythm.



**Table 1.** Results of the registration process per patient

Patient	Age	Gender	No. of Mapping points	Distance between mapping points and MSCT (mm)		
				Mean	SD	Range
1	64	M	217	2.2	1.8	0.0 - 9.1
2	56	M	204	2.2	1.7	0.0 - 9.3
3	58	M	185	1.9	1.4	0.0 - 6.7
4	54	M	220	2.8	1.8	0.0 - 8.3
5	43	M	248	2.1	1.5	0.1 - 7.4
6	56	M	328	2.0	1.6	0.0 - 7.1
7	51	M	117	1.7	1.2	0.0 - 4.9
8	58	F	151	1.9	1.3	0.0 - 6.5
9	55	M	165	1.9	1.5	0.0 - 7.1
10	58	M	316	2.2	1.6	0.0 - 9.9
11	35	M	294	2.3	1.7	0.0 - 7.9
12	65	M	219	2.4	1.5	0.0 - 5.6
13	56	M	282	2.1	1.4	0.0 - 6.3
14	56	M	245	1.9	1.2	0.0 - 5.1
15	56	M	205	2.1	1.7	0.0 - 8.9
16	50	M	191	2.0	1.4	0.0 - 6.8
<b>Mean</b>	53.7		224.2	2.1		
<b>SD</b>	7.2		59.0	0.2		

## DISCUSSION

The results of this study illustrate the feasibility of fusion of MSCT images with 3D electroanatomic mapping in patients undergoing catheter ablation for AF. The mean distance between the MSCT image and the electroanatomic map was only 2 mm, allowing accurate visualization of the catheter position on real surface anatomy during the ablation procedure. The integration of MSCT images and 3D electroanatomic mapping is a promising technique which may facilitate ablation procedures.

### Image processing and registration

The introduction of 3D electroanatomic mapping systems has facilitated the anatomical based ablation procedures for AF (10). However, the surrogate anatomy is reconstructed from multiple catheter recordings along the endocardium (13). Therefore, the use of reconstructed maps may be limited by the complex anatomy of the left atrium and pulmonary veins.

Registration of previously acquired 3D images is a new technique, which offers the ability of using real surface anatomy to guide anatomical based catheter ablation procedures (14,15). Reddy et al (15) demonstrated the feasibility of fusion of magnetic resonance images and 3D electroanatomic mapping in an animal study. After manual segmentation of the magnetic resonance image of the left ventricle, the authors performed a similar registration process. Mean distance between the electroanatomic map and the surface image of the left ventricle was  $4.9 \pm 1.8$  mm. The registration process was limited by the rotation of the left ventricle around its

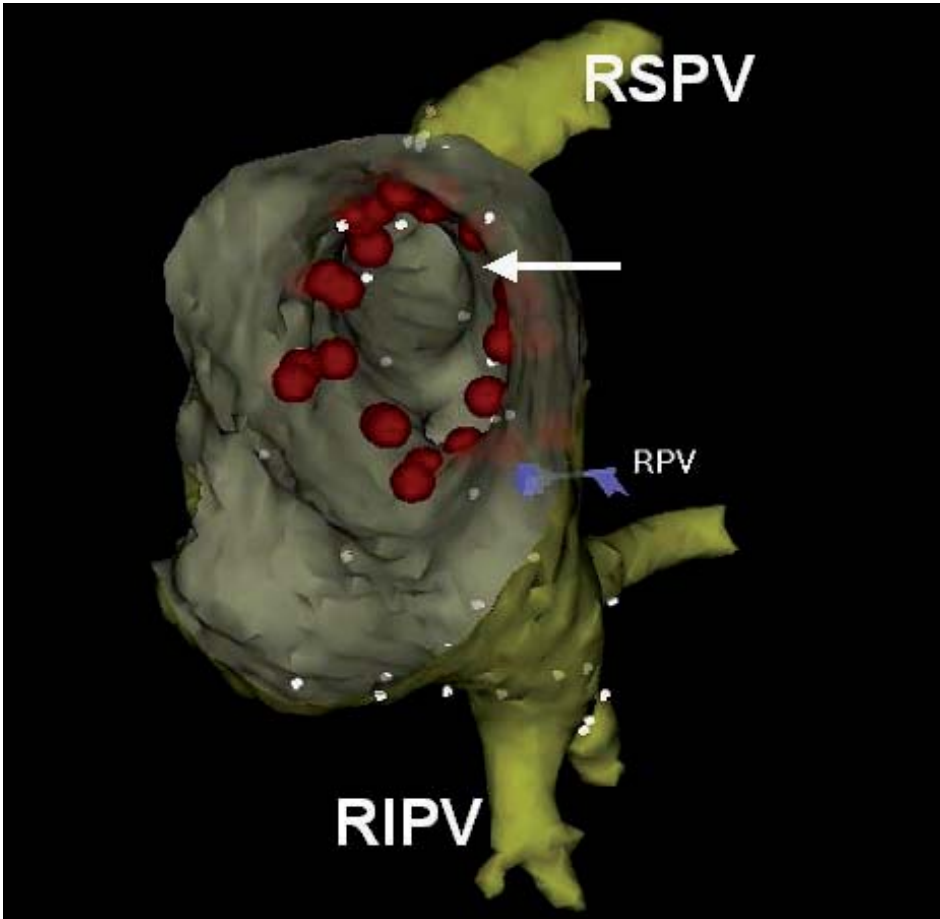


**Figure 3.** After registration, the fused electroanatomic map and MSCT surface image are used to guide catheter ablation. In this view from inside the left atrium, the ostium (arrow) of the right superior pulmonary vein (RSPV) is visualized. Radiofrequency current was applied outside the ostia of the pulmonary veins. Red tags indicate sites of radiofrequency current delivery. RPV = landmark used for registration; RSPV = right superior pulmonary vein; RIPV = right inferior pulmonary vein.

symmetric long axis. To assess an accurate registration, part of the ascending aorta had to be included in the electroanatomic map (15). In the current study, the mean distance between the MSCT image and the electroanatomic map was only  $2.1 \pm 0.2$  mm for the patient group as a whole. Furthermore, the specific anatomy of the left atrium and the pulmonary veins made improper registration due to rotation impossible. The current *in vivo* study demonstrates that fusion of previously acquired MSCT images of the left atrium and 3D electroanatomic mapping can be performed accurately.

### Clinical implications

Anatomy-based catheter ablation for AF is nowadays a safe procedure, and is performed in a large number of centers worldwide (5). Infrequent serious complications, such as pulmonary

vein stenosis, have been reported (16). MSCT can accurately depict the anatomy of the left atrium and the pulmonary veins (8,17), and complications can be avoided to some extent by integration of pre-procedural acquired MSCT images and the 3D mapping images. Furthermore, isolation of all pulmonary veins is necessary to achieve good long-term results. The number and anatomy of the pulmonary veins can be highly variable (18), and the small right middle pulmonary vein has been associated with the initiation of AF (19). Using the electroanatomic mapping system alone, additional or small pulmonary veins are difficult to identify. Detailed information on number, location and branching pattern of all pulmonary veins (as provided by MSCT) during the ablation procedure may improve outcome.

Furthermore, the use of integration of different imaging modalities may reduce procedure time and fluoroscopy time. The introduction of non-fluoroscopic systems reduced fluoroscopy time during AF ablation procedures. However, incorrect geometry of the reconstructed anatomy may limit the use of non-fluoroscopy systems (20). Recently, stereotactic systems have become available to guide ablation procedures (21,22). Although initial results are promising, the high costs of stereotactic systems limit their use in clinical practice. Alternatively, fusion of MSCT images and 3D electroanatomic mapping is easy to perform as demonstrated in the current study and allows visualization of real surface anatomy during the ablation procedure.

### **Limitations**

The present study has some limitations. Scanning was performed during breath-hold, whereas patients were breathing normally during the ablation procedure. Furthermore, heart rate is variable during the ablation procedure. As a consequence, different volumes of the left atrium during the MSCT scan and the ablation procedure may limit the fusion process. However, using a 64-slice MSCT scanner, data acquisition was completed in only 4 seconds. This short breath-hold may minimize the possible difference in left atrial volumes. Reddy et al (15) also observed differences in volume between the surface image and the electroanatomic map of the left ventricle. This resulted in a mean distance of approximately 5 mm between the magnetic resonance surface image and the electroanatomic map. However, ablation based on the magnetic resonance surface image alone resulted in exact ablation lesions in their porcine model (15). We speculate that volume differences in the left atrium and pulmonary veins may be smaller than in the left ventricle, limiting the possible error and allowing precise ablation. Furthermore, the mean distance between the MSCT surface image and the electroanatomic map was only  $2.1 \pm 0.2$  mm for the patient group as a whole. More validation studies in well-controlled animal models are needed to fully appreciate the strengths and limitations of this new fusion approach.

## CONCLUSION

The current study demonstrates that integration of pre-procedural acquired MSCT images and the 3D electroanatomic mapping system can be performed accurately. This new technique allows the use of real surface anatomy to guide anatomy-based catheter ablation procedures. The fusion of different imaging modalities may facilitate catheter ablation for AF.

## REFERENCES

1. Haissaguerre M, Jais P, Shah DC et al. Spontaneous initiation of atrial fibrillation by ectopic beats originating in the pulmonary veins. *N Engl J Med* 1998;339:659-66.
2. Oral H, Scharf C, Chugh A et al. Catheter ablation for paroxysmal atrial fibrillation: segmental pulmonary vein ostial ablation versus left atrial ablation. *Circulation* 2003;108:2355-60.
3. Pappone C, Rosanio S, Oreto G et al. Circumferential radiofrequency ablation of pulmonary vein ostia: A new anatomic approach for curing atrial fibrillation. *Circulation* 2000;102:2619-28.
4. Pappone C, Rosanio S, Augello G et al. Mortality, morbidity, and quality of life after circumferential pulmonary vein ablation for atrial fibrillation: outcomes from a controlled nonrandomized long-term study. *J Am Coll Cardiol* 2003;42:185-97.
5. Cappato R, Calkins H, Chen SA et al. Worldwide survey on the methods, efficacy, and safety of catheter ablation for human atrial fibrillation. *Circulation* 2005;111:1100-5.
6. Ghaye B, Szapiro D, Dacher JN et al. Percutaneous ablation for atrial fibrillation: the role of cross-sectional imaging. *Radiographics* 2003;23:S19-S33.
7. Mansour M, Holmvang G, Sosnovik D et al. Assessment of pulmonary vein anatomic variability by magnetic resonance imaging: implications for catheter ablation techniques for atrial fibrillation. *J Cardiovasc Electrophysiol* 2004;15:387-93.
8. Jongbloed MR, Dirksen MS, Bax JJ et al. Atrial fibrillation: multi-detector row CT of pulmonary vein anatomy prior to radiofrequency catheter ablation--initial experience. *Radiology* 2005;234:702-9.
9. Schwartzman D, Lacomis J, Wigginton WG. Characterization of left atrium and distal pulmonary vein morphology using multidimensional computed tomography. *J Am Coll Cardiol* 2003;41:1349-57.
10. Packer DL. Evolution of mapping and anatomic imaging of cardiac arrhythmias. *Pacing Clin Electrophysiol* 2004;27:1026-49.
11. Dickfeld T, Dong J, Solomon SB et al. Assessment of position error of catheter mapping system (Bio-sense Carto® V8) with CT/MR image integration capabilities. *Heart Rhythm* 2005;2:S278.
12. Jongbloed MR, Schaliij MJ, Zeppenfeld K, Oemrawsingh PV, van der Wall EE, Bax JJ. Clinical applications of intracardiac echocardiography in interventional procedures. *Heart* 2005;91:981-90.
13. Gepstein L, Hayam G, Ben Haim SA. A novel method for nonfluoroscopic catheter-based electroanatomical mapping of the heart. In vitro and in vivo accuracy results. *Circulation* 1997;95:1611-22.
14. Sra J, Krum D, Hare J et al. Feasibility and validation of registration of three-dimensional left atrial models derived from computed tomography with a noncontact cardiac mapping system. *Heart Rhythm* 2005;2:55-63.
15. Reddy VY, Malchano ZJ, Holmvang G et al. Integration of cardiac magnetic resonance imaging with three-dimensional electroanatomic mapping to guide left ventricular catheter manipulation: feasibility in a porcine model of healed myocardial infarction. *J Am Coll Cardiol* 2004;44:2202-13.
16. Packer DL, Keelan P, Munger TM et al. Clinical presentation, investigation, and management of pulmonary vein stenosis complicating ablation for atrial fibrillation. *Circulation* 2005;111:546-54.
17. Cronin P, Sneider MB, Kazerooni EA et al. MDCT of the left atrium and pulmonary veins in planning radiofrequency ablation for atrial fibrillation: a how-to guide. *AJR Am J Roentgenol* 2004;183:767-78.
18. Marom EM, Herndon JE, Kim YH, McAdams HP. Variations in pulmonary venous drainage to the left atrium: implications for radiofrequency ablation. *Radiology* 2004;230:824-9.
19. Tsao HM, Wu MH, Yu WC et al. Role of right middle pulmonary vein in patients with paroxysmal atrial fibrillation. *J Cardiovasc Electrophysiol* 2001;12:1353-7.
20. Rotter M, Takahashi Y, Sanders P et al. Reduction of fluoroscopy exposure and procedure duration during ablation of atrial fibrillation using a novel anatomical navigation system. *Eur Heart J* 2005.
21. Dickfeld T, Calkins H, Zviman M et al. Anatomic stereotactic catheter ablation on three-dimensional magnetic resonance images in real time. *Circulation* 2003;108:2407-13.
22. Solomon SB, Dickfeld T, Calkins H. Real-time cardiac catheter navigation on three-dimensional CT images. *J Interv Card Electrophysiol* 2003;8:27-36.